Transition Metals for Selective Chemical Vapor Deposition of Parylene-Based Polymers

Kathleen M. Vaeth and Klavs F. Jensen*

Department of Chemical Engineering, Massachusetts Institute of Technology, Cambridge, Massachusetts 02139

Received October 13, 1999. Revised Manuscript Received March 8, 2000

A novel method for realizing selective growth of parylene-N and parylene-C synthesized by chemical vapor deposition is presented. Exposure of surfaces to transition metals, metal salts, and organometallic complexes, such as those of iron, ruthenium, platinum, palladium, copper, and silver, is found to inhibit polymer deposition on the substrate. The maximum thickness of the selectively grown polymer films is dependent on the monomer delivery rate to the surface and metal inhibitor used, and for lower growth rates on surfaces patterned with iron, structures 1.4 μm and 4.1 μm in thickness are realized for parylene-N and parylene-C, respectively. The selectively deposited polymer films show no overgrowth onto the metallized areas of the substrate and the slope of the feature sidewalls is steeper than 1.1.μm/μm. Once polymer nucleation finally occurs on the metal films, the morphology of the deposited polymer layer reflects the effectiveness of the metal in preventing polymer deposition. For substrates with little effect on polymer deposition the film morphology consists of uniformly distributed small nodules reflecting multiple polymer nucleation sites on the surface. When the metal initially inhibits polymer growth, the morphology has significantly larger grains, indicating fewer nucleation sites. Possible mechanisms underlying the selective growth are discussed.

Introduction

Polymers are attractive materials for use in thin film applications due to their wide range of mechanical, electrical, and optical properties that can be engineered to fit specific needs. One broad class of polymers that has shown promise for integration into complex devices is parylene and its derivatives. Parylenes are easily prepared by chemical vapor deposition (CVD) of [2.2]-paracyclophanes (Figure 1A), resulting in uniform, pinhole-free coatings at the exclusion of solvents and oxygen.[1−3] The conformal nature of the deposited film with parylene CVD has led to use of the material for moisture barrier layers in circuit boards,[1] corrosion-resistant coatings in archival preservation,[4] and bio-passivation coatings in medical implants.[5] Other potential applications for parylenes include waveguides and coatings for optical systems,[6] acoustic matching layers for transducers,[7] components of microelectrical-mechanical systems (MEMS) such as membranes and channel walls,[8,9] and low dielectric constant materials for multileveled integrated circuits.[4,10] In addition, through modification of the CVD monomer, parylene chemistry can also be used for synthesis of poly(*p*-phenylenevinylene) (PPV),[11,12] which is one of the most promising classes of semiconducting light-emitting polymers.[13,14] Integration of the polymer into more complicated device geometries often requires formation of a patterned film on the substrate, rather than a continuous coating. For parylenes, definition of the polymer layer is typically realized by patterning the film after deposition with reactive ion etching (RIE).[15,16] Although exposure of the organic layer to RIE processing can enhance some properties, such as adhesion of subsequently deposited metals, the harsh environment can also have undesirable side effects such as surface roughening, redeposition of the polymer on the substrate, or degradation in polymer integrity.[10] Patterned parylene films have also been fabricated by direct photopolymerization of a predeposited [2.2]paracyclo-

(1) Gorham, W. F.; Yeh, J. T. C. *J. Org. Chem.* **1965**, *34*, 2366.
(2) Gorham, W. F. *J. Polym. Sci.: Part A-1* **1966**, *4*, 3027.
(3) Lu, T. M.; Moore, J. A. *MRS Bull.* **1997**, *22*, 28.
(4) You, L.; Yang, G. R.; Lang, C. I.; Wu, P.; Moore, J. A.; McDonald, J. F.; Lu, T. M. *J. Vacuum Sci. Technol. A* **1993**, *11*, 3047.
(5) Nichols, M. F. *Crit. Rev. Biomed. Eng.* **1994**, *22*, 39.
(6) Gaynor, J.; Desu, S. B. *J. Mater. Res.* **1994**, *9*, 3125.
(7) Thiagarajn, S.; Martin, R. W.; Proctor, A.; Jayawadena, I.; Sinverstein, F. *IEEE Trans. Ultrason. Ferroelectrics Freq. Control* **1997**, *44*, 1172.
(8) Burns, M. A.; Johnson, B. N.; Brahmasandra, S. N.; Handique, K.; Webster, J. R.; Krishnan, M.; Sammarco, T. S.; Man, P. M.; Jones, D.; Heldsinger, D.; Mastrangelo, C. H.; Burke, D. T. *Science* **1998**, *282*, 484.
(9) Yang, X.; Grosjean, C.; Tai, Y.-C. Solid-State Sensor and Actuator Workshop; Hilton Head Island, SC, June 8−11, 1998; 316.
(10) Majid, N.; Dabral, S.; McDonald, J. F. *J. Electron. Mater.* **1988**, *18*, 301.
(11) Iwatsuki, S.; Kubo, M.; Kumeuchi, T. *Chem. Lett.* **1991**, 1071.
(12) Staring, E. G. J.; Braun, D.; Rikken, G. L. J. A.; Demandt, R. J. C. E.; Kessener, Y. A. R. R.; Bauwmans, M.; Broer, D. *Synth. Met.* **1994**, *67*, 71.
(13) Burroughes, J. H.; Bradley, D. D. C.; Brown, A. R.; Marks, R. N.; Macay, K.; Friend, R. H.; Burns, P. L.; Holmes, A. B. *Nature* **1990**, *347*, 539.
(14) Braun, D.; Heeger, A. J. *Appl. Phys. Lett.* **1991**, *58*, 1982.
(15) Tacito, R. D.; Steinbruchel, C. *J. Electrochem. Soc.* **1995**, *143*, 1974.
(16) Yeh, J. T. C.; Grebe, K. R. *J. Vacuum Sci. Technol. A* **1983**, *1*, 604.

10.1021/cm990642p CCC: $19.00
Published on Web 04/18/2000

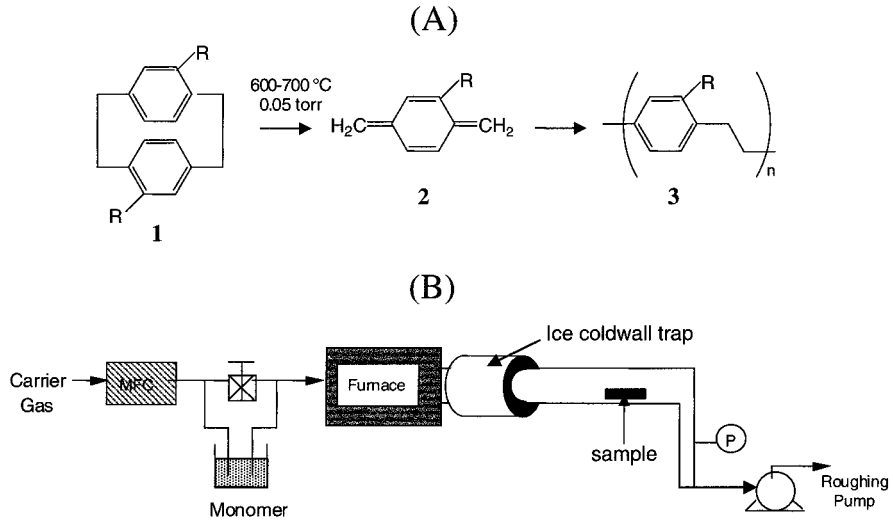

Figure 1. (A) Chemistry for CVD of parylene-N (R═H) and parylene-C (R═Cl) and (B) diagram of reactor used for parylene CVD.

phane layer, but feature thicknesses are limited by the penetration depth of the UV radiation (~1000 Å).[17]

Most of the research and development efforts for parylene-based chemistry have concentrated on two areas: understanding the gas-phase reactions of the monomer;[2,4] and tuning the chemical structure of the polymer to optimize properties such as film adhesion,[18−20] thermal stability,[21] and dielectric constant.[4,22] Much less attention has focused on understanding how the *p*-xylylene reactive intermediate (**2** in Figure 1A) interacts with the deposition surface, and how this interaction influences the growth of the polymer. Such interactions can have an important impact on the structure of the film. For example, for both parylene and PPV prepared by CVD, the aromatic ring of the polymer chain orients parallel to the polymer/metal interface during deposition.[23,24] In addition, when parylene-N is deposited on a cleaved alkali-halide salt surface, nucleation is initiated at the step sites on the substrate.[25] The ability to completely control polymer initiation and propagation reactions in these systems would allow patterned growth of the CVD polymer in a manner analogous to selective deposition of inorganic semiconductors.[26] There have been a few reports of inhibition of parylene growth on surfaces through proper surface design, such as exposing the a silicon surface to a halogen-based plasma,[27] or using thin-film transistors to locally heat areas of the substrate above the critical surface temperature for polymerization.[28] However, these approaches are somewhat cumbersome, and not necessarily compatible with a broad range of substrates or device structures. Recently, we showed that application of a thin layer of iron or iron salt on a surface inhibits the deposition of PPV prepared by parlyene-based CVD chemistry.[29] By patterning the iron on the growth surface, one-step selective deposition of polymeric structures with lateral dimensions on the order of a few micrometers are easily realized on a variety of substrates. In this report, we show that certain evaporated transition metals, metal salts, and organometallic complexes can also be used to inhibit the growth of the CVD polymers parylene-N and parylene-C on surfaces, and explore the nature of metal/*p*-xylylene interaction in detail.

Experimental Section

Polymer Chemical Vapor Deposition. A diagram of the reaction system used for polymer CVD is shown in Figure 1B. The system consists of a monomer delivery zone, pyrolysis zone, and deposition zone. The monomer is placed in a glass tube, heated to 70−90 °C, and transported at low pressures (~0.05 Torr, as measured with a Baratron 0−10 mTorr pressure gauge with ±0.001 Torr sensitivity) to a tube furnace (1 in. diameter quartz tube) by an argon carrier gas (8 sccm, less than 2 ppm of H_2O/O_2). Use of a carrier gas allowed low reactive monomer concentrations to be achieved during polymer deposition, and in all cases, the partial pressure of the gas-phase monomer was kept below 0.001 Torr. This results in a "feed-limited" operation of the reactor i.e., the polymer growth rate is controlled by the monomer delivery rate, with faster film growth observed at higher monomer delivery rates. The monomers used for parylene-N and parylene-C CVD were [2.2]paracyclophane (Sigma-Aldrich) and dichloro[2.2]paracyclophane (courtesy of Specialty Coating Systems), respectively. Upon pyrolysis, these monomers yield a *p*-xylylene reactive intermediate (Figure 1A), which is transported to the deposition zone (1 in. diameter glass tube) in heated lines (T > 95 °C) to minimize polymer deposition on the walls of the transport zone. Under normal conditions, the *p*-xylylene adsorbs onto surfaces below a critical temperature and polymerizes. Typical growth conditions for the polymer films were temperatures of 675 and 25 °C for the furnace and deposition zones respectively, and growth rates of 4−35 Å/s.

(17) R. P. Mariella, J.; Steinhauser, S. W.; Diebold, A. C. *J. Vacuum Sci. Technol. B* **1987**, *5*, 1360.
(18) Yamagishi, F. G. *Thin Solid Films* **1991**, *202*, 39−50.
(19) Sharma, A. K.; Yasuda, H. *J. Vacuum Sci. Technol.* **1982**, *21*, 994.
(20) Beach, W. F.; Lee, C.; Basset, D. R.; Austin, T. M.; Olson, R. *Encyclopedia of Polymer Science & Engineering*; Wiley: New York, 1985; Vol. 17.
(21) Ganguli, S.; Agrawal, H.; Wang, B.; McDonald, J. F.; Lu, T.-M.; Yang, G. R.; Gill, W. *J. Vacuum Sci. Technol. A* **1997**, *15*, 3138.
(22) Senkevich, J. J.; Desu, S. B. *Appl. Phys. Lett.* **1998**, *72*, 258.
(23) Niegisch, W. D. *J. Appl. Phys.* **1967**, *38*, 4110.
(24) Vaeth, K. M.; Jensen, K. F. *Adv. Mater.* **1997**, *9*, 490.
(25) Isoda, S. *Polymer* **1984**, *25*, 615.
(26) Coleman, J. J.; Lammert, R. M.; Osowski, M. L.; Jones, A. M. *IEEE J. Selected Top. Quantum Electron.* **1997**, *3*, 874.
(27) U.S. Patent #5,618,379, International Business Machines Corporation, 1997.
(28) Sabeti, R.; Charlson, E. M.; Charson, E. J. *Polym. Commun.* **1989**, *30*, 166.
(29) Vaeth, K. M.; Jensen, K. F. *Adv. Mater.* **1999**, *11*, 814.

Evaporation and Patterning of Metal Growth Inhibitors. All of the metal growth inhibitors were deposited by electron-beam evaporation (2 Å/s), with the exception of silver and gold, which were deposited by thermal evaporation (10 Å/s), in chambers with a base pressure of 9×10^{-8} Torr. The evaporated metal was defined on the surface using a poly(dimethylsiloxane) (PDMS) elastomeric membrane as a shadow mask,[30] or by photolithography (primarily iron). The thickness of the evaporated metal films was 25 Å, as measured by atomic force microscopy. All substrates were exposed to air prior to deposition, and X-ray photoelectron spectroscopy analysis showed that all of the metallized surfaces possessed a native oxide, with the exception of platinum and gold (as expected). For photolithographic patterning of the metal layers, the substrate was coated with photoresist (Shipley Microposit 1813), exposed to UV light with a Zeiss contact aligner, and developed (Shipley MF-319 developer). Metal was then evaporated onto the surface, and the remaining photoresist was removed with a standard liftoff in acetone, or subjected to a UV flood exposure and removed with developer. During polymer CVD, film growth only occurred on the metal-free areas of the surface.

Treatment of Surfaces with Metal Inhibitors Deposited from Solution. All salts and organometallic complexes were purchased from Sigma-Aldrich, with the exception of fluorochromium phthalocyanine (Alfa Aesar), and used without further purification. The metal salts were deposited onto surfaces by dipping the substrate into an aqueous solution of metal salt (0.2 g/mL) for 20 s and then drying the surface in a stream of filtered nitrogen gas. The organometallic complexes were applied to the surface by placing a drop of a solution or suspension of the complex in hexanes or toluene on the surface (0.05 g/mL), and allowing the solvent to evaporate. Note that some of the organometallic complexes used, such as nickel and fluorochromium phthalocyanine, are suspected carcinogens, and should be handled with appropriate protective equipment.

Polymer Film Characterization. The polymer films were characterized ex-situ by infrared reflection−absorption spectroscopy (IRRAS) with a Nicolet 800 spectrometer. Polymer morphology was characterized with a Digital Nanoscope 3000 Atomic Force microscope (AFM) in tapping mode, and film thicknesses were measured with a Tencor P-10 surface profilometer with a tip radius of 2 μm.

Results and Discussion

Iron Inhibition of CVD Polymer Growth. Our previous experience with inhibition of CVD PPV growth with iron suggests that there is a direct interaction between the metal and halogenated *p*-xylylene reactive intermediate that prevents the initiation and propagation steps of polymerization from occurring.[29] To further explore the interaction between *p*-xylylenes and iron, the growth of CVD parylene-C and parylene-N, which are also formed via *p*-xylylene derivative intermediates, on iron-treated surfaces was investigated. Shown in Figure 2 is an IRRAS spectra taken ex-situ of parylene-C deposited at a rate of 10 Å/s on two aluminized substrates run side-by-side in the deposition chamber. Prior to polymer deposition, 25 Å of iron was evaporated onto one of the aluminum surfaces (Fe/Al), while the other was left untreated (Al). On the Al surface (Figure 2A), parylene-C deposition is clearly detected with IRRAS, and profilometry (not shown) reveals a polymer thickness on the order of 2000 Å. This same thickness is observed on a silicon control surface run with the samples, which indicates that the effect of aluminum and silicon on polymer deposition is approximately equal. However, on the Fe/Al surface, no deposition of polymer or other species is detected (Figure 2B). Therefore, as with PPV deposited by CVD, the presence of iron on the growth surface leads to inhibition of parylene-C deposition. This same trend is observed with parylene-N on Al and Fe/Al surfaces. Inhibition of parylene-C growth continued until 1.7 μm of polymer deposited on the Al substrate, after which polymer growth was also observed on the Fe/Al surface. The IRRAS spectrum of the polymer that does eventually deposit on the iron-treated substrate (Figure 2C) is very similar to that of parylene-C on the Al surface. Therefore, the iron layer appears to delay polymerization on the surface, rather than catalyzing the decomposition of the *p*-xylylene to a different solid material.

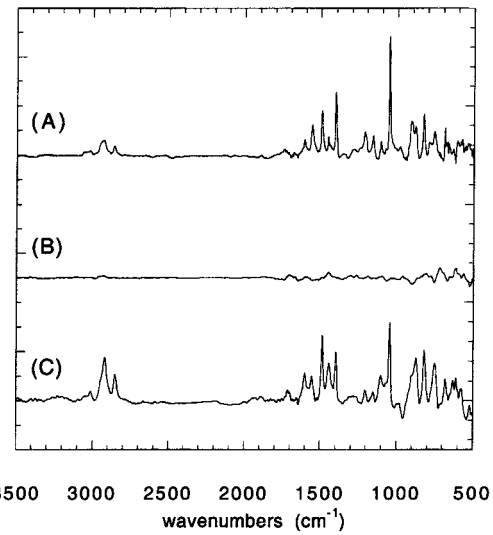

Figure 2. IRRAS spectra of (A) Al surface and (B) Fe/Al surface run together in a parylene-C deposition. (C) IRRAS spectra of polymer that does eventually grow on Fe/Al surface.

By patterning iron on a silicon surface with photolithography, micrometer-scaled selectively grown parylene structures with sharp feature definition were realized. Shown in Figure 3A is profilometry of parylene-C features grown at a rate of 10 Å/s on a silicon substrate. The structures are 10 μm in width and periodicity, which is in agreement with the mask used for the photolithography, and 1.5 μm in height, with no loss in selectivity of the growth (selectivity loss occurred after deposition of 1.7 μm of polymer). From the profilometry scan, the slope of the feature sidewalls is calculated to be 1.1 μm/μm, which we consider to be a lower limit due to convolution of the profilometer tip geometry with the feature edge for this film thickness.[31] For the same reaction conditions, the maximum selectively grown thickness of parylene-N realized with an iron growth inhibitor was 6000 Å before loss of selectivity occurred (Figure 3B), which is significantly less than that of parylene-C. Although the maximum selectively grown thickness achieved with each polymer did depend on the substrate and reactor cleanliness (i.e., if the reaction chamber was free of unreacted monomer and substrate free of photoresist residue), for the same reaction conditions, this difference in degree of selectivity between the two polymers was consistently observed.

(30) Jackman, R. J.; Duffy, D. C.; Cherniavskaya, O.; Whitesides, G. M. *Langmuir* **1999**, *15*, 2873.

(31) Tencor P-10 Surface Profiler Reference, Pub. #412937-27 Rev A p 3−4; Software Version 3.1; Tencor Instruments: Santa Clara, 1996; p 3.

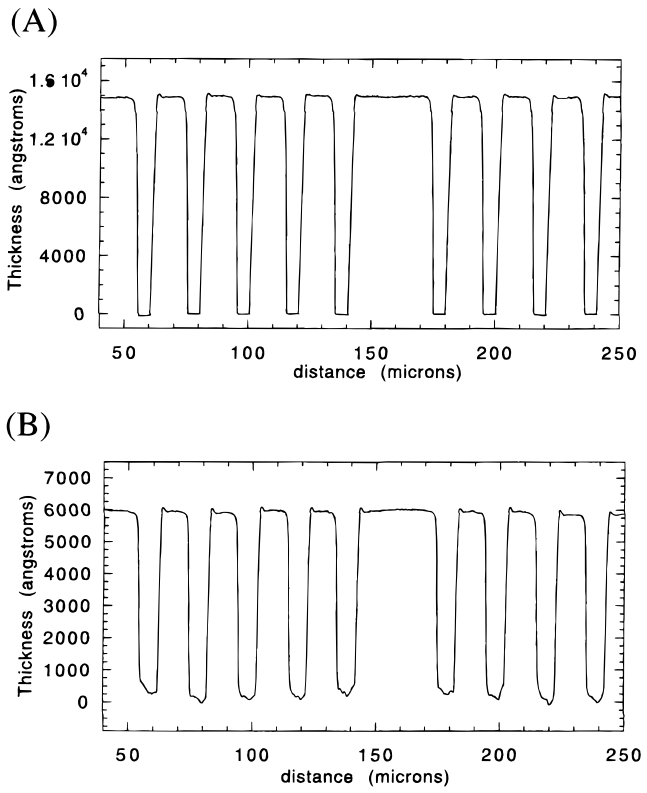

Figure 3. Selective growth of (A) parylene-C and (B) parylene-N with an iron inhibitor patterned by photolithography for a growth rate of 10 Å/s.

The maximum thickness of selectively grown polymer achieved with parylene-N and parylene-C on iron is significantly greater than that of CVD PPV prepared from α,α′-dichloro *p*-xylenes, which is typically not more than 3500 Å for a single run.[29] This difference could be caused by the halide placement on the end group of the *p*-xylylene in CVD PPV chemistry, as opposed to its location on the ring of the *p*-xylylene in parylene-C deposition or not at all in parylene-N chemistry. Alternatively, this effect could reflect differences in the cleanliness of monomer pyrolysis with the two chemistries, since pyrolysis of [2.2]paracyclophanes is very clean and efficient[2], while that of α,α′-dichloro-*p*-xylenes is known to have side products that could contaminate the iron surface and facilitate polymer deposition.[32] The greater growth selectivity observed with parylene-C as compared to parylene-N on iron-treated surfaces is more of a direct reflection of the differences in surface chemistry occurring with the two systems, since both polymers are prepared from the clean [2.2]paracyclophane chemistry.

Selective Polymer Growth with Solution-Based Iron Inhibitors. In addition to evaporated iron, application of iron salts and organo−iron complexes on surfaces also resulted in the inhibition of parylene-N and parylene-C growth, in much the same way we have found them to control the deposition of CVD PPV.[29] With the solution-based inhibitors, the quality of selective growth was highly dependent on how well the metal salt or complex covered the growth surface. Other factors, such as oxidation state of the metal, anion in the iron salt, and steric conditions, appeared to be secondary in importance, with comparable selective growth observed for iron(II) chloride, iron(III) chloride, iron(II) bromide, and iron(II) sulfide, ferrocene, and iron(II) phthalocyanine. Since the organometallic complexes are known to be very stable to oxidation in air, the fact that these materials also inhibit polymer deposition implies that growth inhibition proceeds through an interaction between the *p*-xylylene derivatve and the metal center itself (as opposed to a site on a metal oxide).

Table 1. Maximum Selectively Grown Film Evaporated Thickness of Paryelne-N and Parylene-C on Various Metals for a Polymer Growth Rate of 10 Å/s

metal		maximum selectively grown thickness (Å)	
group	symbol	parylene-N	parylene-C
4	Ti	0	0
5	Ta	400	0
6	Cr	0	0
8	Fe	6000	17000
	Ru	8630	2220
9	Co	700	400
10	Ni	810	220
	Pd	3130	1590
	Pt	5750	2540
11	Cu	3350	850
	Ag	3600	1620
	Au	700	140
12	Zn	0	0
13	Al	0	0
	In	0	0
14	Sn	0	0

The Effectiveness of Other Metals for Inhibition of Parylene Growth. To further explore the metal/*p*-xylylene interaction, the effect of other transition and nontransition metals on parylene-N and parylene-C deposition was examined. In our previous work with CVD PPV, the only other substances found to inhibit polymer deposition were evaporated copper films and ruthenium chloride salts.[29] However, for parylenes prepared from [2.2]paracyclophanes, a broader range of metals were found to delay the initiation and propagation reactions of parylene CVD on surfaces. For example, shown in Figure 4 are surface profilometry and IRRAS spectra of the evolution of parylene-N growth on an aluminum substrate with 400 Å thick silver pads evaporated on the surface. Early in the deposition process, the IRRAS and profilometry show that polymer deposition occurs on the aluminum surface, but not on the silver. Inhibition of polymer growth on the silver continues until roughly 3000 Å of polymer is deposited on the aluminum surface, resulting in a complete reversal of the original surface topography. Eventually, polymer growth also occurs on the silver surface, and the IRRAS spectra of the polymer deposited on the silver is similar to that of parylene-N. The profilometry also reveals that after a significant amount of secondary growth has occurred on the silver surface, there is a decreased polymer growth rate near the interface between the two metals (Figure 4E), which we attribute to perturbations in the reactive monomer concentration in these regions by the feature sidewalls.

Shown in Table 1 is the maximum selective film thickness of parylene-N and parylene-C deposited at a rate of 10 Å/s on a silicon substrate patterned with a variety of metal inhibitors. This maximum thickness can

(32) Vaeth, K. M.; Jensen, K. F. *Macromolecules* **1998**, *31*, 6789.

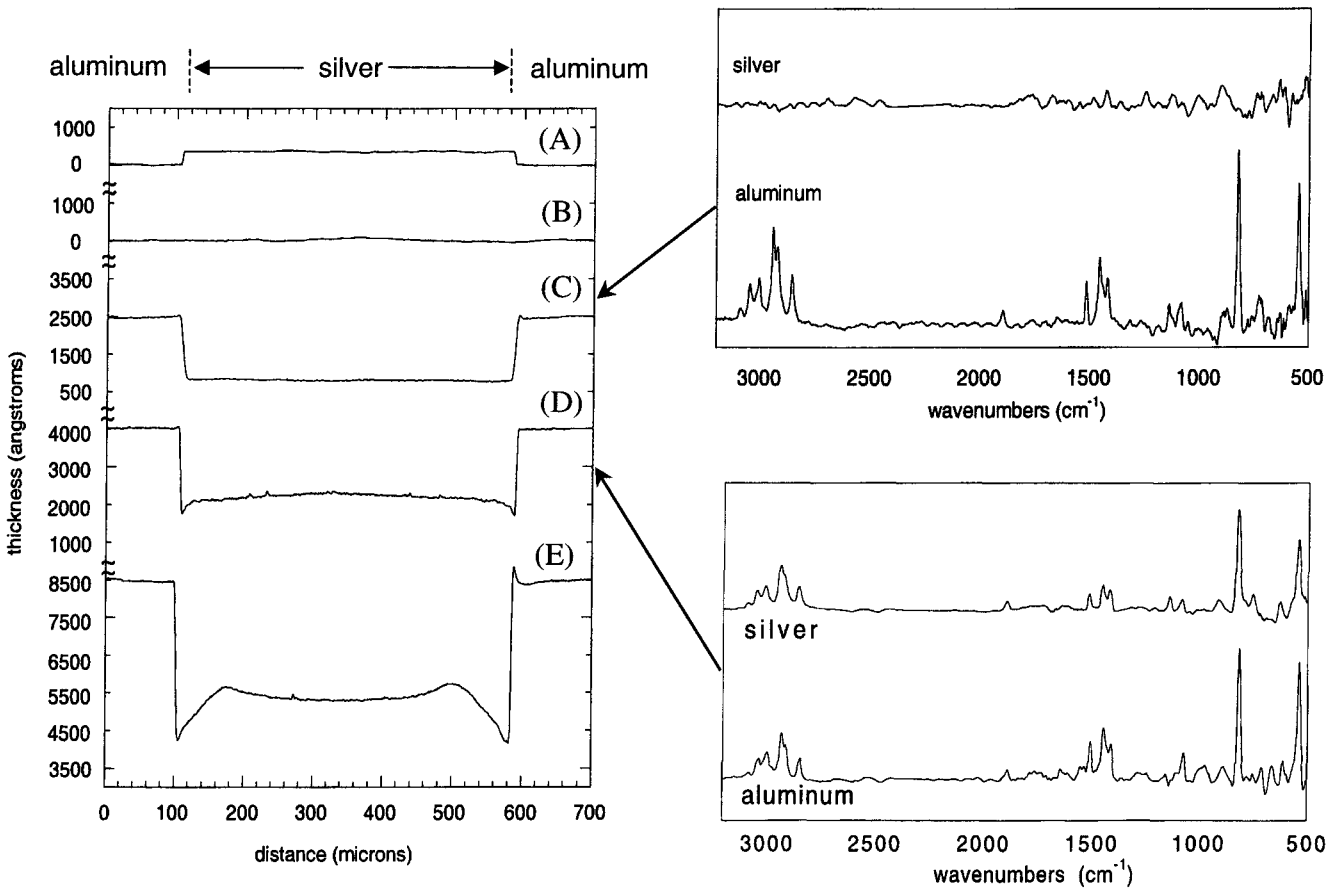

Figure 4. Profile evolution and IRRAS of parylene-N growth on an aluminum surface with 400 Å silver pads: (A) $t = 0$, (B) $t =$ 40 s, (C) $t = 4$ min, (D) $t = 6.5$ min, and (E) $t = 14$ min.

be thought of as an indication of the relative activity of the metal in inhibiting CVD polymer growth. For both polymers, the metals most effective at inhibiting polymer growth are transition metals from group 8 such as iron and ruthenium, followed by platinum, palladium, and nickel from group 10, copper and silver from group 11, cobalt from group 9, and tantalum from group 5. However, metals such as titanium and chromium from groups 4 and 6, as well as zinc from group 12, and nontransition metals such as aluminum, magnesium, indium, and tin, do not significantly inhibit polymer growth. For the reaction conditions used, iron was the most effective inhibitor of parylene-C growth, but ruthenium was actually more active than iron in preventing parylene-N deposition on surfaces. In addition, with the exception of iron, the maximum selectively grown polymer thickness for a given metal inhibitor was greater for parylene-N than parylene-C.

In addition to evaporated metals, salts and organometallic complexes of other transition metals were effective at inhibiting polymer deposition. In particular, ruthenium(III) chloride and metal phthalocyanines such as vanadyl and manganese phthalocyanine prevented the deposition of both parylene-N and parylene-C on surfaces, while phthalocyanines of other metals, such as those of cobalt, copper, and zinc, exhibited a small inhibiting effect on parylene-N deposition, but no effect on parylene-C. Application of other metal salts or complexes on the growth surface, such as sulfates of calcium, cobalt, chromium, magnesium, manganese, nickel, silver, and zinc, chlorides of platinum, lithium, and sodium, as well as titanyl, fluorochromium, and nickel phthalocyanine did not have a significant inhibiting effect on the growth of either polymer.

Mechanism of the Growth Inhibition Process. The lack of polymer overgrowth from the metal-free areas of the substrate onto the metal-treated regions indicates that the metal layer suppresses both the initiation *and* propagation reactions of polymerization on the surface. Otherwise, a growing polymer chain in a metal-free area could initiate polymer growth at the edges of the metal-treated regions on the substrate. Prevention of both initiation and propagation reactions would occur if the *p*-xylylene is not available for polymerization on these surfaces, either because the molecule did not adsorb on the metal surface (i.e., small sticking coefficient), or if the *p*-xylylene interacts with the metal in such a way that it is deactivated while adsorbed. Since deposition of both polymers does eventually occur on the metal-treated surfaces, deactivation of the molecule is more likely, rendering it unavailable for polymerization. Although the exact mechanism for deactivation of the *p*-xylylene is not known at this time, possible pathways include simple binding or complexation of the molecule to the metal, or conversion of the *p*-xylylene to [2.2]paracyclophane derivatives, *p*-xylene derivatives, or hydrocarbon fragments by the metal (the latter of which is considered unlikely at the mild temperature of 25 °C used for polymer deposition). For the purposes of the following discussion, the byproducts of the metal/*p*-xylylene interaction will simply be referred to as "deactivated *p*-xylylene". A simple diagram showing how monomer adsorption and polymerization would proceed on transition metal-treated and untreated surfaces with

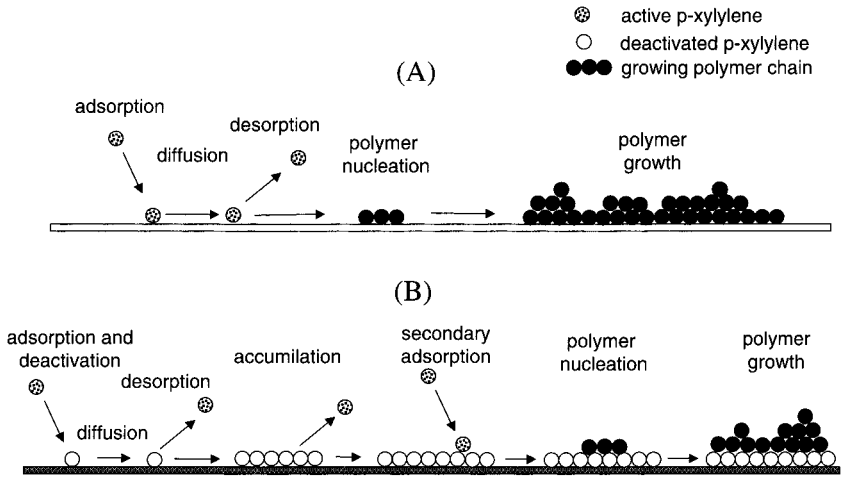

Figure 5. Steps for monomer adsorption and polymerization on (A) untreated substrates and (B) transition metal-treated substrates. Note the accumulation of deactivated *p*-xylylene on the metal surface

such a deactivation process is given in Figure 5. On the untreated surface (Figure 5A), polymer nucleation occurs after a few monomers adsorb onto the surface and come into contact with each other, and polymer propagation then proceeds in a normal fashion. However, on the metal-treated substrate (Figure 5B), the monomers that directly adsorb onto the surface are deactivated to nucleation and propagation reactions by the metal. In this case, polymerization can only proceed if secondary monomer adsorption takes place on top of the deactivated layer. Therefore, the accumulation of deactivated *p*-xylylene on the surface would control the extent to which the metal layer delays polymerization, with breakdown of selectivity occurring after a critical concentration of deactivated molecules has accumulated (X_{crit}).

The rate of accumulation of deactivated *p*-xylylene on the metal-treated surface can generally be described as follows:

$$dX/dt = C - k_d X \quad (1)$$

where X is the concentration of deactivated *p*-xylylene on the metal, C is the effective monomer delivery rate to the surface, and k_d is the rate constant for desorption of deactivated *p*-xylylene from the metal surface. If the deactivated *p*-xylylene does not desorb quickly from the metal surface ($k_d \ll 1$), then the concentration of adsorbed species would be a linear function of time with slope C. In this case, the maximum selectively grown polymer film thickness attainable would not vary with monomer delivery rate, since the same number of molecules would be required to reach X_{crit} irrespective of growth rate, resulting in loss of selectivity. However, if the deactivated *p*-xylylene desorbs from the metal surface easily, as shown in Figure 6, accumulation of the deactivated species is controlled by the rates of monomer delivery and desorption to and from the surface as follows:

$$X = (C/k_d)(1 - \exp(-k_d t)) \quad (2)$$

In this case, the deactivated *p*-xylylene concentration on the surface asymptotically reaches a steady-state value (C/k_d), and the maximum thickness of selectively grown polymer attainable is influenced by the monomer

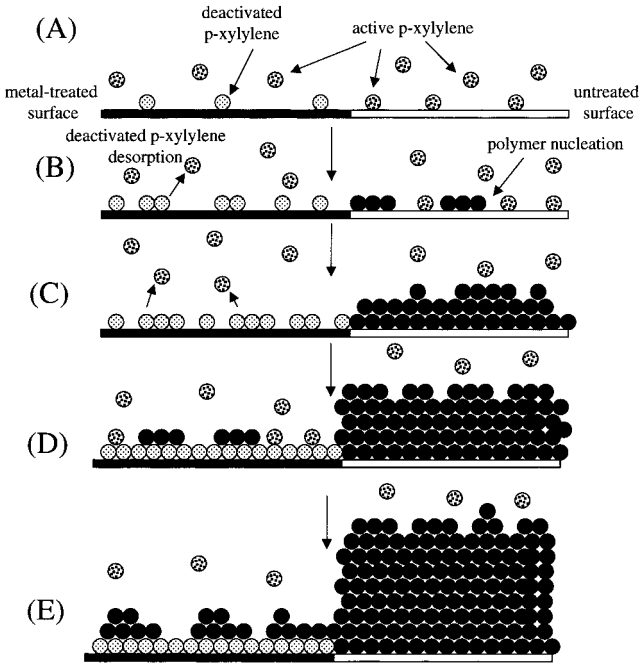

Figure 6. Interaction of *p*-xylylene and metal (A) $t \approx 0$, shortly after monomer delivery starts; (B) $t = t_1$, polymer nucleation begins on untreated surface, but not on the treated surface; (C) $t = t_2$, the deactivated *p*-xylylene slowly accumulates on metal-treated surface, while film growth proceeds rapidly on untreated surface; (D) $t = t_3$, $X \approx X_{crit}$ the critical concentration of deactivated *p*-xylylene is reached on treated surface, allowing polymer growth to commence; and (E) selectivity loss on metal-treated surface as film growth proceeds.

delivery rate. At higher monomer delivery rates, deactivated *p*-xylylene desorption may not balance monomer delivery, and X_{crit} would be reached fairly quickly. As the rate of monomer delivery is decreased, the flux to the surface becomes close or equal to that of deactivated *p*-xylylene desorption, resulting in a slower accumulation of deactivated *p*-xylylenes on the surface. This allows more time for the polymer to deposit in the untreated regions of the substrate before loss in selectivity occurs. Below a certain monomer delivery rate, the steady-state concentration of deactivated *p*-xylylene on the surface would be lower than X_{crit}, and selectivity loss would never be realized.

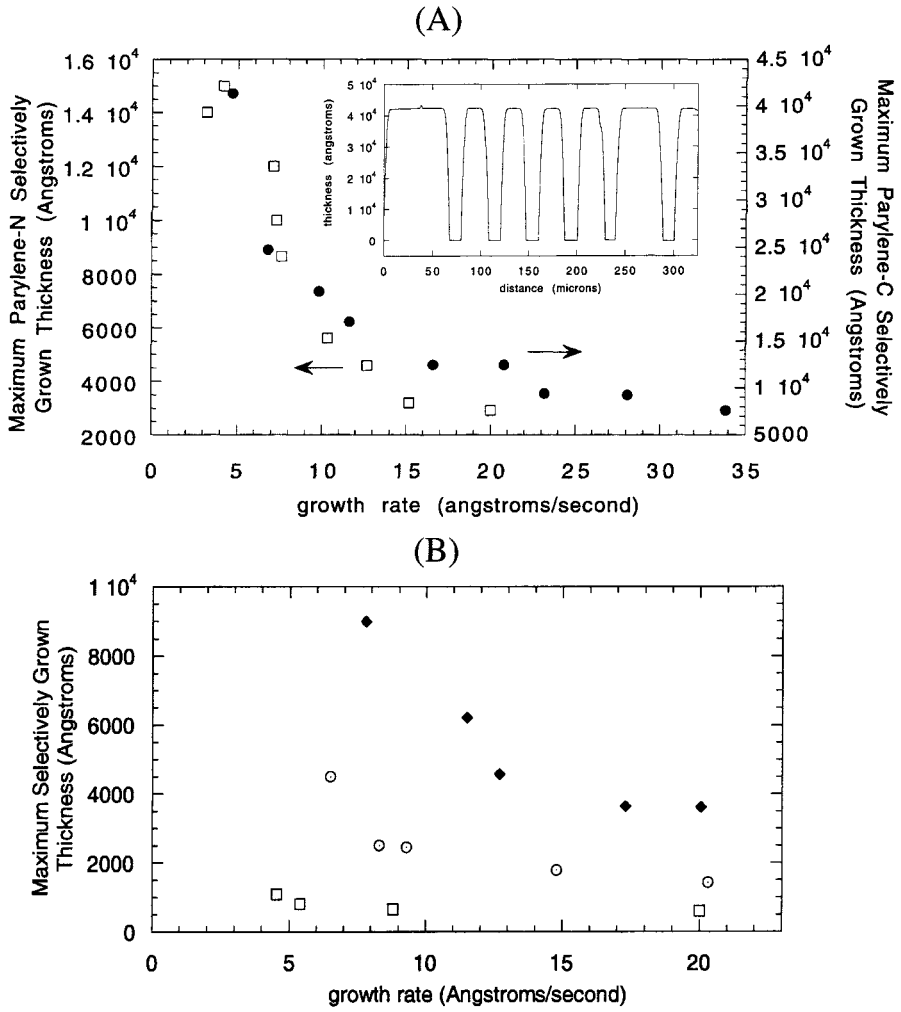

Figure 7. Maximum selectively grown polymer thickness as a function of growth rate for (A) parylene-N (open squares) and parylene-C (solid circles) with an iron inhibitor (profilometry of parylene-C features grown selectively with an iron inhibitor shown in inset), and (B) parylene-N (open squares) and parylene-C (solid circles) with a copper inhibitor, and parylene-N (solid diamonds) with a platinum inhibitor.

To probe the nature of the deactivated *p*-xylylene on the metal-treated surface, the effect of monomer delivery rate (as reflected by the growth rate of the polymer for the feed-limited operation of the deposition system) on the maximum selectively grown polymer thickness attainable was investigated. The maximum selective thickness of both parylene-N and parylene-C as a function of polymer growth rate on a silicon substrate with metal-treated regions is shown in Figure 7. On iron-treated surfaces (Figure 7A), the maximum selectively grown film thickness was found to increase slowly with decreasing polymer growth rate until a growth rates of 15 Å/s for both polymers. Below this rate, the maximum thickness realized increases more rapidly, with films over 1 and 4 μm in thickness achieved for parylene-N and parylene-C, respectively. Profilometry of the thickest features grown to date is shown in the inset of Figure 7A (4.1 μm parylene-C). Similar trends are observed with other metals (Figure 7B), although the effect is more pronounced with metals that have a greater relative activity in inhibiting polymer growth. Therefore, the deactivated *p*-xylylene must desorb fairly easily from the transition metal-treated surface, as described in the simple scheme in Figure 6. Presumably, the rates of monomer delivery and desorption are more balanced at the lower growth rates, resulting in slower accumulation of deactivated *p*-xylylene on the surface, which allows thicker features to be deposited in the untreated regions of the substrate.

Once polymer nucleation finally occurs on the metal films, the morphology of the deposited polymer layer reflects the effectiveness of the metal in preventing polymer deposition. Shown in Figure 8 are AFM images of parylene-N deposited at 10 Å/s onto several metal surfaces after loss of selectivity occurs (note that all metals were exposed to air prior to polymer deposition, and, with the exception of platinum, had native oxides on the surface). For metals such as aluminum, which have little effect on polymer deposition, the film morphology consists of many grains or nodules that are fairly uniformly distributed across the surface. This suggests that there are multiple polymer nucleation sites on the surface, which form many small polymer islands that coalesce to form a continuous layer (Figure 9A). As the relative activity of the metal in inhibiting polymer growth increases (Ni < Ag < Pt < Fe), these nodules become larger in size and less uniformly distributed, resulting in a more open-film morphology. This correlation between the dimensions of the morphology structure and the ability of the metal to inhibit polymer deposition suggests that as the inhibition activity of the metal increases, there are fewer nucle-

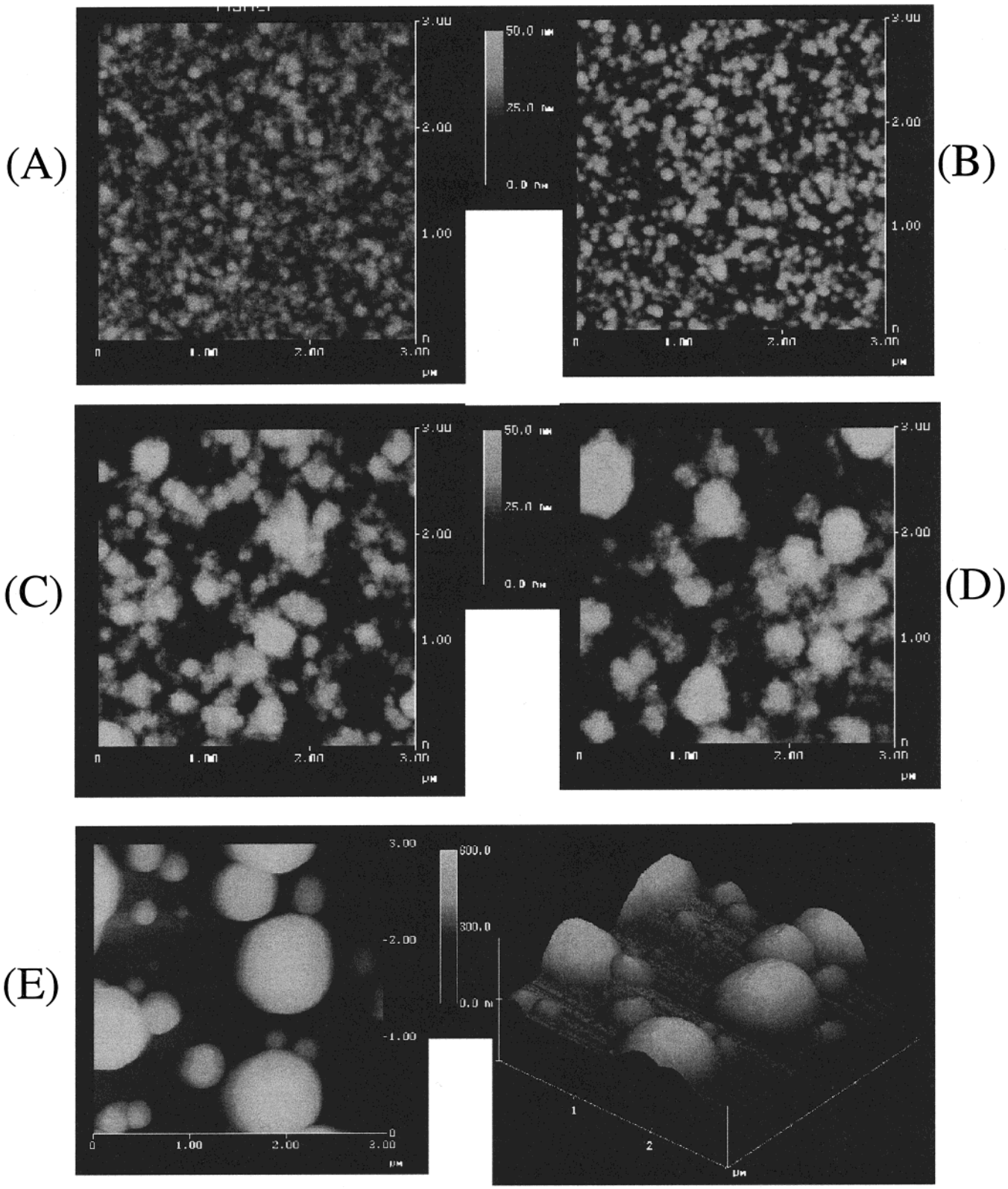

Figure 8. AFM scans of parylene-N deposition after loss of selectivity on (A) aluminum, (B) nickel, (C) silver, (D) platinum, and (E) iron.

ation sites for growth. This leads to the formation of fewer islands, which have to grow to larger sizes before coalescence (Figure 9B). Note in particular the morphology of the polymer deposited on the iron surface (Figure 8E), which is completely islandlike in nature, suggesting that the polymerization reaction is starved for reactive *p*-xylylene on the surface. In fact, these islands tend to grow upward, reaching a height of over 5000 Å without coalescing, which would suggest that the best source of reactive *p*-xylylene for a growing polymer chain on the iron surface is a molecule from the gas phase that directly adsorbs onto the island.

Since evaporated metals, metal salts, and organometallic complexes are all effective at inhibiting polymer growth, and the conditions used for polymer deposition are relatively mild (25 °C), the types of complexes that

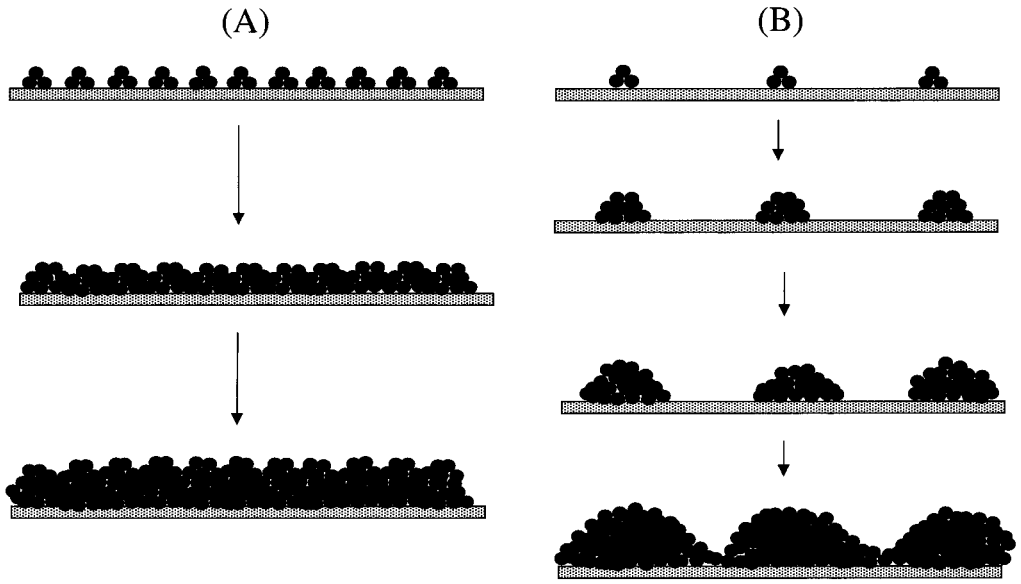

Figure 9. Schematic for polymer film nucleation and coalescence for surfaces which (A) do not and (B) do inhibit polymer deposition (spheres represent monomers).

transition metals form with organic aromatic systems in solution may provide a good model for the nature of the passivation interaction between the metal and the *p*-xylylene. It is well-known that *p*-xylylenes exist in two forms—a lower energy singlet state, which possesses a quinoid-like geometry, and a higher energy biradical triplet state.[33] At room temperature, practically all of the *p*-xylylenes in the reaction system exist in the singlet state. However, calculations of the electronic structure of singlet *p*-xylylene reveal that there is a significant biradical component to the state (as high as 40%),[34] which presumably allows the molecule to be reactive enough for polymerization to proceed. It is possible that when *p*-xylylene adsorbs on the metal surface, the molecule interacts with the metal in such a way that the biradical component of the structure is quenched, thereby preventing it from participating in the initiation and propagation reactions of the polymerization process. All of the metals found to show some effectiveness at inhibiting polymer growth are also known to interact with conjugated systems similar to the end groups of *p*-xylylene, such as η^3-allyl or η^4-trimethylenemethane-like complexes. In fact, synthesis and characterization of bis(tricarbonyliron) *p*-xylylenes, in which iron forms a η^4-trimethylenemethane-like complex on either side of the molecule with a portion of the ring and end group of the *p*-xylylene, has been reported.[35] A similar type of interaction between the iron and *p*-xylylene on the growth surface would reduce the biradical character of the molecule, and prevent it from polymerizing.

Conclusions

The discovery that the growth of parylene-N and parylene-C can be inhibited by treating the deposition surface with transition metals, transition metal salts and organo-transition metal complexes is a completely new approach for fabricating patterned films of these materials and has important implications for integration of these films into complex device structures. Use of an inhibitor creates a powerful tool, allowing selective CVD polymer growth on wide variety of substrates. Such a one-step patterning approach for selective growth of parylene-based polymers may aid their utilization as low dielectric constant materials in dual damascene-type integrated circuits, components of MEMS-based systems, and materials for photonic crystals.

Acknowledgment. The authors acknowledge the Fannie and John Hertz Foundation and the DARPA MicroFlumes Program for partial funding for this research, as well as the MRSCC shared facilities supported by NSF (DMR-9400334), Mr. Gale Petrich for support with the electron-beam evaporator, Dr. Rebecca Jackman, Dr. David Duffy, and Professor George Whitesides for the elastomeric membranes, and Specialty Coating Systems for providing the dichloro[2.2]paracyclophane monomer.

CM990642P

(33) Szwarc, M. *Disc. Faraday Soc.* **1947**, *2*, 46.
(34) Hiberty, P. C.; Karafiloglou, P. *Theor. Chim. Acta* **1982**, *61*, 171.
(35) Koray, A. R.; Krieger, C.; Staab, H. A. *Angew. Chem., Int. Ed. Engl.* **1985**, *24*, 521.